ORIGINAL SCIENTIFIC PAPER OPEN ACCESS

Thermal stress analysis in hot rolling process

Taiwo Olajide Hazeez[1], Gbeminiyi Mufutau Sobamowo[1], Ibrahim Ademola Fetuga[1*], Uchechukwu Charles Modebelu[2], Sodiq Adewale Adeleke[1], Kolade Sodeeq Aderemi[1]

[1] University of Lagos, Department of Mechanical Engineering, Lagos, Nigeria

[2] Bowie State University, Department of Management Information Systems, Maryland, United State of America

ARTICLE INFO

[*] **Correspondence:** fetugaebraheem@gmail.com

DOI: 10.5937/engtoday2300017H

UDC: 621(497.11) **ISSN:** 2812-9474

Article history: Received 27 September 2023; Revised 1 November 2023; Accepted 10 November 2023

ABSTRACT

In continuous hot slab rolling, it is important to know the temperature distribution within the strip along the length of the rolling mill because the dominant parameter controlling the kinetics of metallurgical transformations and the flow stress of a rolled metal is temperature. A mathematical model based on finite difference method is utilized to predict the temperature distribution and microstructural changes during the continuous hot slab rolling process. The effects of various parameters such as heat of deformation, the work-roll temperature, the rolling speed, and the heat transfer coefficient between the work-roll and the metal were all taken into account in the analysis. From the parametric analysis carried out, it was shown that the temperature in the deformation zone increases as the percentage reduction in the strip thickness and the rolling process, it affects the temperature distribution in the work-roll significantly, the heat generation on the strip-roll interface increases significantly when the percentage reduction in the strip exceeds a certain value. It was also shown that at low rolling speed, the temperature increase is uniform inside the strip and the roll and the maximum temperature of the strip occurs in the neighborhood of the strip centerline region.

KEYWORDS

Hot rolling process, Stress, Angular position, Strip temperature, Deformation zone, Strip velocity, Percentage drop, Strip thickness.

1. INTRODUCTION

Flat-shaped items are made using a commercial procedure known as “continuous hot slab rolling”. To mitigate flow-stress, and improve the rolled metal working properties, heat is applied to the material in order to reach its working temperature in the first step of this process [1]. Due to the metallurgical requirements placed on the output, the material is typically hot rolled above the transformation temperature and then removed from the last stand above this temperature. In order to achieve the desired sheet thickness, several work-roll sets are used to make a sheet out of the slab with satisfactory dimensions, following the homogenization of the slab's temperature distribution in a reheat furnace. When the slab is rolled into the roughing stand, it is referred to as a "strip". The work-roll is, however, often just referred to as "the roll", for simplicity. After that, the run-out table is used to forcefully cool the strip in order to regulate its structure and shape and due to a reasonable concern for mill productivity. Phase change takes place during cooling. The unequal distribution of temperature across the strip generates significant thermal stress during

cooling, especially when the temperature is in the transformation range. The steel strip experiences local plastic deformation due to the extreme heat stress, which then adds residual tension. Given that the rolled metal's flow stress is strongly correlated with the temperature in this operation, temperature dispersion in the metal affects metal flow and roll-force [2].

During the hot rolling process of steel and aluminum, the work-rolls are exposed to significant temperature increases, complex cyclic temperature transients accumulate within the work-rolls, particularly near the surface. In a bid to assess the process parameters and the composition of the work piece, knowing the temperature in the roll gap is crucial.

The rolls are typically cooled to prevent overheating, as is widely recognized. The center of the roll seems to have a constant temperature, while cyclic temperature transients only appear near the surface. This "boundary-layer" behavior is the primary cause of temperature-stresses of the roll and assists in transferring heat to the rolls via a metal that is heated.

Since the roll surface heats up from contact with the heated strip and loses heat as it cools from contact with the air and water over a revolution, rolls with many revolutions will experience cyclic compressive and tensile loads along their circumference. Repeated thermal tensile pressures widen the microcracks on the surface of the roll. Due to this, the rolled product's surface quality deteriorates, it is recommended that the rolling process be halted so that the rolls can be replaced. As a result, the rolls' time of operation (i.e., their duration spent in operation) diminish. In order to prevent the emergence of microcracks and so lengthen the roll life, it is crucial to comprehend temperature advancement and the resulting thermal stress changes in the roll. Investigations into hot-mill "pacing," which is concerned with managing the rate at which slabs run through a hot mill, served as the first motivation for research of temperature effects. To guarantee that the metallurgical requirements of the completed product are satisfied, one important goal of pacing is to attain specific slab temperatures at different locations throughout the mill. Numerical models that depict heat transfers between slabs and rolls when rolling is crucial for predicting temperatures because they can be incorporated into a complete mill simulation for design studies and, in clarified forms, "in on-line control."

Understanding the temperature is necessary for quantitative evaluation of the process variables and the physical makeup of the workpiece since it is one of the factors that most affects how materials behave during hot rolling. Hot rolling modeling has recently been the subject of several studies and publications; their ranges span from modern, complex finite element approaches to extremely simplified closed solutions [3–9]. To study three-dimensional strain in rolling, Nagpal devised a general stream equation [10]. For determining the required energy, Marques and Martins developed an upper bound method based on Nagpal's double stream function [11]. For the hot rolling process, Chung et al. [12] utilized a streamline coordinate FDM to predict the distributions of dislocation density, pressure, and temperature. A FDM (Finite-difference model) in single-dimension and homogeneous deformation were adopted by Hollander [13] to determine the temperature field in hot-rolling. So as to predict the velocity field under isothermal, constant and plane strain rolling conditions that are unsteady, Mori et al. [14] used a rigid-plastic and partially compressible material assumption. Lenard and Hwu [15] evaluated the work-roll deformation effect on strain fields during flat rolling using FEM (finite-element method). Yarita et al. [16] used a finite element model that was elastic-plastic in nature to study the rolling process of the plain strain. Employing an updated lagrangian code, attempts were made to correctly forecast the distribution of engineering stress and engineering strain inside the area of deformation. In their study [17,18] Hwang et al. evaluated the process of rolling heated strip. Rolled metal temperature dispersion, strain field and work-roll temperature dispersion were determined. As Devadas and Samarasekara [19] predicted, temperatures vary in the work-roll and also within the heated strip metal that was rolled. They have investigated how process parameters affect the temperature field in their work. In their paper, the kinetics of oxidation of iron during the process of hot rolling was also studied. In numerous studies [20–23], temperature fields have been analyzed during hot rolling. In a few articles [24,25], temperature fluctuations in work-rolls were discussed. Teseng [25] evaluated the fluctuations in temperature within the work-rolls as part of their analysis of the distribution of thermal stress in rolls, while Sluzalec [24] used a finite element approach in two-dimensions to forecast how temperatures vary during hot rolling. Boguslaw and Cierniak [26] investigated the fluctuation of temperature while hot rolling using a two-dimensional model. Karagiozis and Lenard discussed temperature distributions when a hot slab rolling in a single-pass and the consequencet of several variables on inhomogeneity of temperature in their paper [27]. Sassani and Xiao [28] calculated the distribution of temperature during the hot flat-rolling of materials with profiles that are curved. To forecast the spread in temperature in the metal that was rolled, they used a sub-model for temperature that relied on transient heat transfer in either one- or two- dimensions. To forecast the distributions in temperature and flow of metal when rolling, Chen et al. [29] utilized the finite element and finite difference approaches in two-dimensions. The phase change kinetics, temperature distribution and grain size during hot rolling, also the velocity field in the area of deformation, were calculated using a finite element approach in two-dimensions [30]. Sarajevan [31] suggested a mathematical model. Then, in order to correlate the fluctuations in strain rate and temperature on the deforming metal flow behavior, he connected the model suggested with a finite element model that is thermo-visco-plastic. This method accurately predicted a temperature field that agreed well with the findings of experiments. Using the finite element method, together with Avitzur's upper bound method, Sarajevan [32] employed a straightforward

model to estimate temperature. Pawelski [33] solved the heat transfer equation analytically connecting the strip and work-roll analytically so as to determine the coefficient of transfer of heat in the area. The coefficient was a function of scale thickness, roll-bite contact duration, the roll and strip physical characteristics, and roll speed. In the solution, some boundary conditions could not be taken into account, so the thermal crown of the work-roll could not be accurately predicted. In order to forecast the transient temperature field and the work rollers thermal profile in the rolling of the hot strip, an axisymmetric model in two-dimensions created using the finite difference approach was proposed [34]. Ginzburg [35] created the guiding concepts for rolling mill computer simulation. His simulation resulted in enhanced product quality, reduced energy use, and optimal manufacturing conditions. In order to identify the ideal working circumstances, During the rolling process, Ginzburg [34] investigated the main factors influencing temperature variation and strategies to prevent heat loss between the stands (roughing stands and finishing stands), and discovered that temperature changes are largely caused by losses resulting from convection and radiation, heat transfer to rollers by convection, spraying of water for removing oxides, as well as temperature increases resulting from thermal balance in primary work zones and also the backup rolls with axisymmetric thermal fields that take into account the transfer of heat between strips, rolls, coolant, and the surrounding environment. Mei et al. [36] created a program in which he employed the finite element approach to ascertain the dispersion of temperature when hot rolling. Analysis was done on the thermal resistance, cooling of water, and air-cooling transfer of heat coefficients interconnecting the strip and work-roll. Hadala and Malinowski [37] presented an enhanced heat transfer model. An estimate made at a commercial steel factory validated the concept. Water usage needs to be tracked to ensure accurate temperature forecasts in online management systems. The authors suggested that the water flowing from the roller cooling system influences plate cooling. Due to the heat gained by the rollers and the heat dissipation from the surface of the strip, there was an approximated 13% temperature drop in the plate. Khadem [38] investigated the heat transmission in a strip traveling through a transfer table with a thermal shield and also without a thermal shield. He used a finite difference approach to analyze an energy balance in two-dimensions and calculate the amount of heat the strip losses. Because of the upper surface's high temperature, the convective transfer of heat from it was believed to combine in this method.

An important industrial process for producing flat-shaped objects is hot slab rolling, where a hot slab is mechanically processed using rotating work-rolls on varying stands. To accurately anticipate the lifespan of the work-rolls, a precise control of the distribution of temperature within the metal being rolled is essential, prior to and after hot-rolling, knowing the temperature spread within the roll is extremely important. Stresses brought on by changes in the material's temperature might lead to fracture or deformation due to plasticity of the material.

In order to reduce the amount of plastic deformation, it is crucial to research how temperatures and thermal stress affect the materials during rolling. Our understanding of the impacts caused by these temperatures on the working materials will be aided by this study, which will help us establish the actual temperatures of the working rolls and the surfaces at various locations of the material. With this understanding, a variety of techniques can be created and used to decrease the extent of fracturing of materials passing through the rolling process, which reduces costs and also extends the tool and material life.

2. METHODOLOGY

2.1. Descriptions of the rolling processes

In rolling as shown in Figure 1, the material is squeezed by two rotating rollers as it passes through an opening between the rollers. After the material has been rolled, its thickness is almost equal to the distance between the rotating rollers. When the shape of the rollers is cylindrical, the material is rolled into a plate or sheet. However, rolling process is not just for flat sheets. In the case of contoured surfaces, the shape can be rolled using rollers that are profiled. If the surface pattern requires more depth than can be achieved in a single rolling pass, multiple rollers can be used. Metals can either be hot or cold rolled, much like in other forming procedures. Rolling a specific amount of material hot or cold results in significantly different microstructures and energy requirements. The yield stress of a metal increases with cooling, meaning that more energy is required to shape it. However, a significant drawback of hot rolling is that it leaves a poor surface-finish, since the air oxidizes the material's surface. Smaller stresses can be used while cold rolling ductile metal. As a result of work hardening at these temperatures, the product can gain strength, which is one benefit. Utilizing polished rollers during cold rolling reduces oxidation and also produces a superior finishing for the surface. Therefore, the cold rolling process is a good finishing method when making plates and sheets. Considering the importance of a smooth finishing on the surface of this product, cold rolling is used to polish steel sheets for vehicle bodywork.

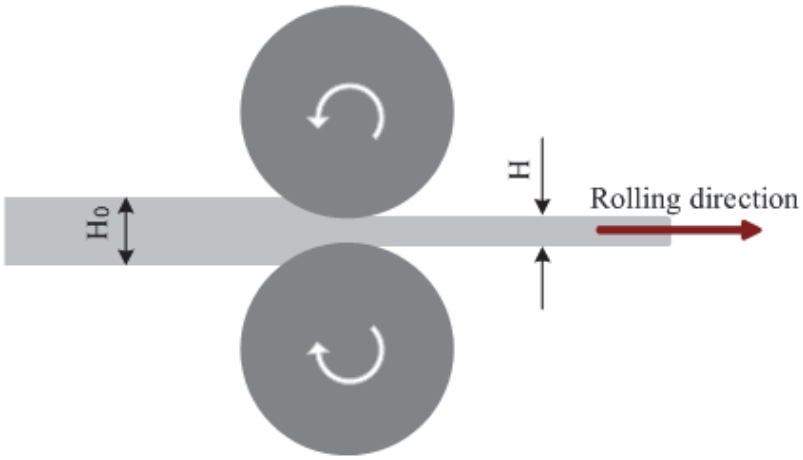

Figure 1: Rolling of a metal

2.2. Model formulation of the rolling process

Transient phase distributions of temperature in the workpiece and work rolls are solved utilizing the physical model for the computational domain in Figure 2 and 3 for the purpose of analyzing the thermal stress distribution in outer and deformation zones of rigid-plastic materials.

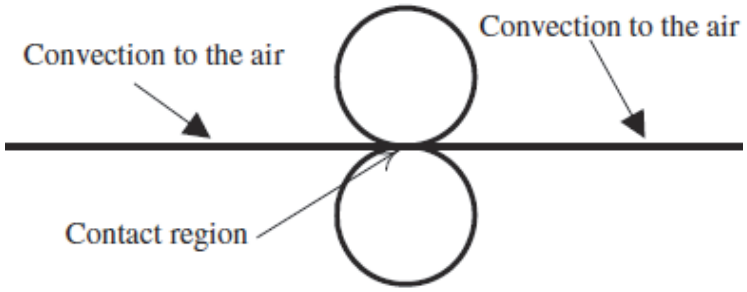

Figure 2: A mechanism for transferring heat during metal rolling

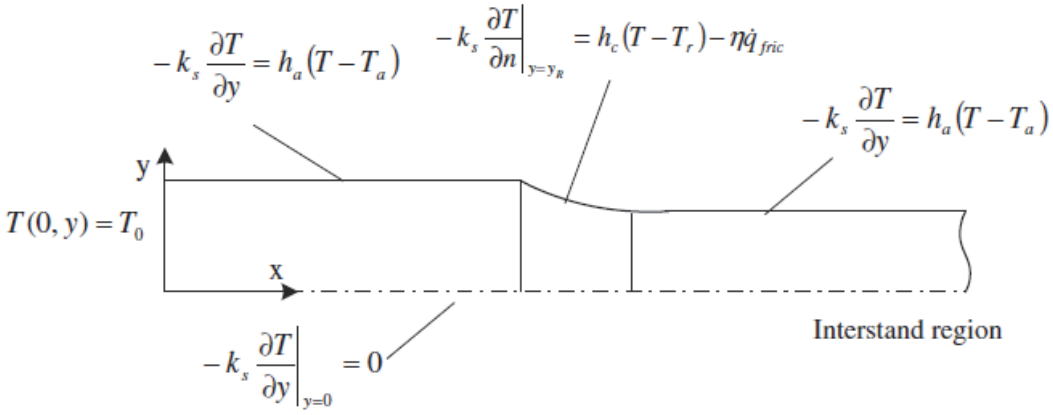

Figure 3: The computational domain of hot rolling

$$\frac{\partial\left(\rho c_p(T)T\right)}{\partial t} + u_x \frac{\partial\left(\rho c_p(T)T\right)}{\partial x} + u_y \frac{\partial\left(\rho c_p(T)T\right)}{\partial y} = \frac{\partial}{\partial x}\left(k(T)\frac{\partial T}{\partial x}\right) + \frac{\partial}{\partial y}\left(k(T)\frac{\partial T}{\partial y}\right) + \dot{q}_{def} + \dot{q}_{fric} \tag{1}$$

Based on frictional slide on the roll/strip interface and volumetric heat of deformation caused by material deformation, we can determine the distributed heat flux by

$$\dot{q}_{def} = \eta \bar{\sigma} \dot{\bar{\varepsilon}} \tag{2}$$

and

$$\dot{q}_{fric} = m\tau |u_r| A \tag{3}$$

The formula for calculating the material's flow stress is

$$\bar{\sigma} = \sigma_0 + B\varepsilon^n \tag{4}$$

where

$$\bar{\varepsilon} = \int_0^L \frac{\dot{\bar{\varepsilon}}}{u_x} dx \tag{5}$$

$$\tau = mk_s\left[\frac{-2}{\pi} arctan\left(\frac{|u_r|}{a}\right)\right], \quad m = \sqrt{\frac{h_f}{R}} \frac{ln\left(\frac{h_o}{h_f}\right) + \frac{1}{4}\sqrt{\frac{h_f}{R}}\sqrt{\left(\frac{h_o}{h_f}\right)-1}}{arctan\left(\sqrt{\left(\frac{h_o}{h_f}\right)-1}\right)} \tag{6}$$

By minimizing the corresponding energy functional in a Eulerian framework and presuming flat strain conditions, the velocity field may be determined. Using Hill's proposed velocity field [22]

$$u_x = \frac{u_0 h_0}{h}, \quad u_0 = \frac{u_n h_n}{h_0} \tag{7}$$

$$u_y = \frac{-y u_0}{h} \frac{d}{dx}\left(\frac{h_0}{h}\right) \tag{8}$$

Then, the thermal model for the rolled material is given as

$$\frac{\partial\left(\rho c_p(T)T\right)}{\partial t} + \left(\frac{u_n h_n}{h}\right)\frac{\partial\left(\rho c_p(T)T\right)}{\partial x} - \frac{y u_0}{h}\frac{d}{dx}\left(\frac{h_0}{h}\right)\frac{\partial\left(\rho c_p(T)T\right)}{\partial y} = \frac{\partial}{\partial x}\left(k(T)\frac{\partial T}{\partial x}\right) + \frac{\partial}{\partial y}\left(k(T)\frac{\partial T}{\partial y}\right) + \dot{q}_{def} + \dot{q}_{fric} \tag{9}$$

where heat generation can be written as;

$$\dot{q}_{def} = \eta\left(\sigma_0 + B\left(\int_0^L \left(\frac{h(x)\dot{\bar{\varepsilon}}}{u_n h_n}\right) dx\right)^n\right)\dot{\bar{\varepsilon}} \tag{10}$$

$$\dot{q}_{fric} = m|u_r| A k_s \sqrt{\frac{h_f}{R}} \frac{ln\left(\frac{h_o}{h_f}\right) + \frac{1}{4}\sqrt{\frac{h_f}{R}}\sqrt{\left(\frac{h_o}{h_f}\right)-1}\left[\frac{-2}{\pi} arctan\left(\frac{|u_r|}{a}\right)\right]}{arctan\left(\sqrt{\left(\frac{h_o}{h_f}\right)-1}\right)} \tag{11}$$

The initial condition is

$$t = 0, \; T = T_o \;\; at \;\; 0 \le x \le L, \; 0 \le y \le y_R \tag{12}$$

The horizontal symmetry plane's thermal boundary condition is

$$t > 0, \; \frac{\partial T}{\partial y} = 0 \;\; at \;\; y = 0, \; 0 \le x \le L \tag{13}$$

At the deformation zone of the upper surface of the material being rolled, where the material is in contact with the roll

$$t > 0, \; -k(T)\frac{\partial T}{\partial y} = h_c\left(T - T_r\right) - \eta\dot{q}_{fric} \;\; at \;\; y = y_R, \; 0 \le x \le L \tag{14}$$

Where the material comes into touch with the air at the surface (top) of the rolled material

$$t > 0, \; -k(T)\frac{\partial T}{\partial y} = h_a\left(T - T_a\right) \;\; at \;\; y = y_{surface}, \; 0 \le x \le L \tag{15}$$

At the entrance into the roll

$$t > 0, \; T = T_o \;\; at \;\; x = 0, \; 0 \le y \le y_R \tag{16}$$

At the exit from the roll

$$t>0,\ \frac{\partial T}{\partial x}=0\ \ at\ \ x=0,\ 0\le y\le y_R \tag{17}$$

where hc is the coefficient of heat transfer at the interface, Tr is the work-roll surface temperature at the point of contact. The ambient temperature (Ta) and the coefficient of heat transfer due to convection (Ha) are different quantities. g is the amount of heat transferred from the contact point to the rolling metal. L is the length of the domain or strip considered, and T0 represents the metal's initial temperature. Outside the deformation zone, the symbol q, which describes the rate of heat generation, is not used. Symbols k, cp denotes the rolling metal's thermal conductivity, density, and specific heat. The variables ux and uy represent longitudinal component and thickness component respectively. The variable hn represent thickness of the neutral point and Vn represent velocity of the neutral point. m is a friction factor constant that depends on h0 and hf, along with radius of work-roll (R). Ks represents yield stress due to shearing of the material, 'a' represents a constant of the order of 10^{-24}[23]; A constant friction coefficient, m, frictional stress, t, the relative velocity between the work-roll and strip, Vr, and the surface of contact, A, are used to calculate the distributed heat flux generated during frictional sliding on the roll/strip interface. The volumetric heat of deformation produced by material deformation is qdef. Table 1 shows the values of these mechanical constants for steel.

2.3. Thermal Modeling of the Roll

Considering the rolls as shown in Figure 3 and 4,

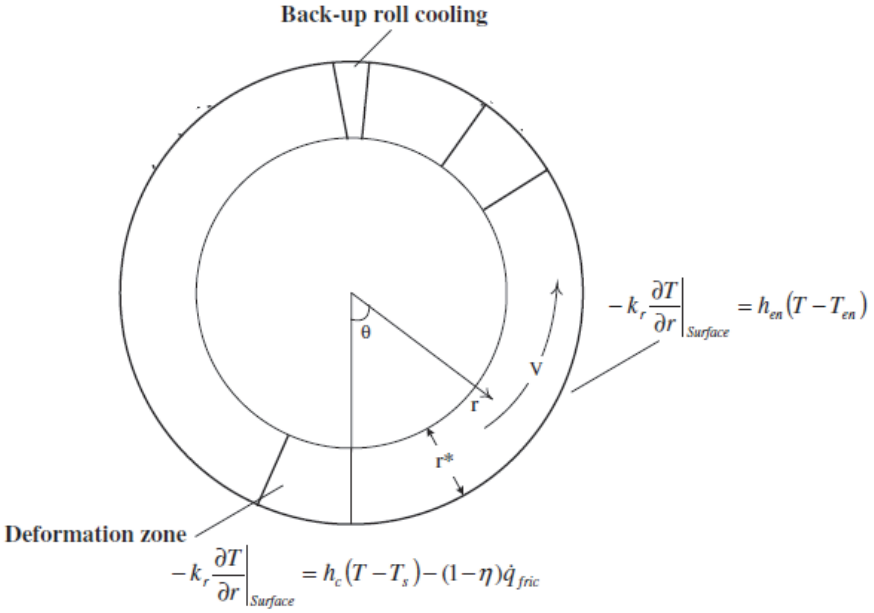

Figure 4: The computational domain of the roll

The work-roll's thermal model is provided as

$$\frac{\partial\left(\rho c_p(T)T\right)}{\partial t}+\omega\frac{\partial\left(\rho_r c_{p,r}(T)T\right)}{\partial\theta}=\frac{1}{r}\frac{\partial}{\partial r}\left(rk_r(T)\frac{\partial T}{\partial r}\right)+\frac{1}{r^2}\frac{\partial}{\partial\theta}\left(k_r(T)\frac{\partial T}{\partial\theta}\right) \tag{18}$$

The initial condition is

$$t=0,\ T=T_o\ \ at\ \ 0\le r\le r_o,\ 0\le\theta\le 2\pi \tag{19}$$

The horizontal symmetry plane's thermal boundary condition is

$$t>0,\ \frac{\partial T}{\partial y}=0\ \ at\ \ y=0,\ 0\le x\le L \tag{20}$$

The input heat flux that travels from the strip contact area to the work-roll is considered as

$$t>0,\ -k(T)\frac{\partial T}{\partial r}=h_c\left(T-T_s\right)-\eta\dot{q}_{fric}\ \ at\ \ r=r_{surface},\ 0\le\theta\le 2\pi \tag{21}$$

Ts represents the temperature of the strips' surface, T represents the surface temperature of the work-roll. The value of 'Ts' can be obtained by resolving the thermal issue posed by the strip.

The work-roll cools down as a result of exposure to the environment, which is taken into account on the work roll's free surface. Due to the rolls contact with the air, the input heat flux transported from the roll is

$$t>0,\ -k(T)\frac{\partial T}{\partial r}=h(T-T_a)\ \ at\ \ r=r_{surface},\ 0\le\theta\le 2\pi \tag{22}$$

At the work-rolls outside layer

$$t>0,\ T=T_o\ \ at\ \ r=r^*,\ 0\le\theta\le 2\pi \tag{23}$$

Table 1: Mechanical properties used in the model

σ_o (MPa)	B (MPa)	N	σ_{oR} (MPa)	E_R (GPa)	υ
337	655	0.24	1200	200	0.3

Table 2: Thermo-physical properties utilized in the model

Physical property	Value
k_s (W/mK)	171.87+0.2015T-2.94 x $10^{-4}T^2$
ρ_s (kg/m^3)	2780
c_s (J/kgK)	1000.08+1.2655T-2.617 x $10^{-3}T^2$
k_r (W/mk)	42.284-3.0052 x 10^{-2}T-1.3509 x $10^{-5}T^2$-4.4298 x $10^{-8}T^3$
ρ_r (kg/m^3)	7850
c_r (J/kgK)	429.47 + 0.2575T -5 x 10^{-5} T^2

2.4. Model formulation of the rolling process

In order to develop the model for the thermal stress distribution in the rolling process, equilibrium equations are used. The rolling process subjected to stress must satisfy the equilibrium equation which was developed from the elasticity theory. For rolled materials

$$\frac{\partial\sigma_{xx}}{\partial x}+\frac{\partial\sigma_{xy}}{\partial y}=0 \tag{24}$$

$$\frac{\partial\sigma_{xy}}{\partial x}+\frac{\partial\sigma_{yy}}{\partial y}=0 \tag{25}$$

Thermal stress can be related with Airy's function using

$$\sigma_{xx}=-\frac{\partial^2\chi}{\partial y^2} \tag{26}$$

$$\sigma_{yy}=-\frac{\partial^2\chi}{\partial x^2} \tag{27}$$

Where χ is the Airy's function which is the summation of

$$\chi=\chi_c+\chi_p \tag{28}$$

$$\nabla^4\chi_c=0\ \text{ and }\ \nabla^2\chi_p=-\alpha E\Delta T \tag{29}$$

After the derivation, the thermal stresses for the isotropic material are

$$\sigma_x=\sigma_y=\frac{\alpha E}{1-\nu}\left[-\Delta T+\frac{1}{h_n}\int_{-h/2}^{h/2}\Delta T dz+\frac{12z}{h_n^3}\int_{-h/2}^{h/2}\Delta T z dz\right] \tag{30}$$

After the derivation, the thermal stresses for the anisotropic material are

$$\sigma_x = \frac{\alpha_x E_x + \alpha_y v_{xy} E_y}{1 - v_{xy} v_{yx}} \left[-\Delta T + \frac{1}{h_n} \int_{-h_n/2}^{h_n/2} \Delta T dy + \frac{12z}{h_n^3} \int_{-h_n/2}^{h_n/2} \Delta T y dy \right] \tag{31}$$

$$\sigma_y = \frac{\alpha_y E_y + \alpha_x v_{xy} E_x}{1 - v_{xy} v_{yx}} \left[-\Delta T + \frac{1}{h_n} \int_{-h_n/2}^{h_n/2} \Delta T dy + \frac{12z}{h_n^3} \int_{-h_n/2}^{h_n/2} \Delta T y dy \right] \tag{32}$$

Where $\Delta T = T(x, y, t) - T_a$

While for the rolls

$$\frac{\partial \sigma_{rr}}{\partial r} + \frac{\partial \sigma_{zr}}{\partial z} + \frac{\sigma_{rr} - \sigma_{\theta\theta}}{r} = 0 \tag{33}$$

$$\frac{\partial \sigma_{zr}}{\partial r} + \frac{\partial \sigma_{zz}}{\partial z} + \frac{\tau_{rz}}{r} = 0 \tag{34}$$

The thermal stress is related to thermal strains with aids of thermoelectricity equations. For the rolled material or strip, they are:

$$\varepsilon_{xx} = \frac{1}{\mathrm{E}} \left[\sigma_{xx} - \upsilon(\sigma_{yy} + \sigma_{zz}) \right] + \alpha \Delta T \tag{35}$$

$$\varepsilon_{yy} = \frac{1}{\mathrm{E}} \left[\sigma_{yy} - \upsilon(\sigma_{xx} + \sigma_{zz}) \right] + \alpha \Delta T \tag{36}$$

$$\varepsilon_{zz} = \frac{1}{E} \left[\sigma_{zz} - \upsilon(\sigma_{xx} + \sigma_{yy}) \right] + \alpha \Delta T \tag{37}$$

While for the rolls

$$\varepsilon_{rr} = \frac{1}{\mathrm{E}} \left[\sigma_{rr} - \upsilon(\sigma_{\theta\theta} + \sigma_{zz}) \right] + \alpha T \tag{38}$$

$$\varepsilon_{\theta\theta} = \frac{1}{\mathrm{E}} \left[\sigma_{\theta\theta} - \upsilon(\sigma_{rr} + \sigma_{zz}) \right] + \alpha T \tag{39}$$

$$\varepsilon_{zz} = \frac{1}{E} \left[\sigma_{zz} - \upsilon(\sigma_{rr} + \sigma_{\theta\theta}) \right] + \alpha T \tag{40}$$

We can write the stress-strain-temperature relation as

$$\sigma_{rr} = \frac{\mathrm{E}}{1 - \upsilon^2} \left[\varepsilon_{rr} + \upsilon(\varepsilon_{\theta\theta} + \varepsilon_{zz}) - (1 + \upsilon) \alpha \Delta T \right] \tag{41}$$

$$\sigma_{\theta\theta} = \frac{\mathrm{E}}{1 - \upsilon^2} \left[\varepsilon_{\theta\theta} + \upsilon(\varepsilon_{zz} + \varepsilon_{rr}) - (1 + \upsilon) \alpha \Delta T \right] \tag{42}$$

$$\sigma_{zz} = \frac{\mathrm{E}}{1 - \upsilon^2} \left[\varepsilon_{zz} + \upsilon(\varepsilon_{r} + \varepsilon_{\theta\theta}) - (1 + \upsilon) \alpha \Delta T \right] = 0 \tag{43}$$

For the rolls

$$\sigma_{rr} = \frac{\mathrm{E}}{1 - \upsilon^2} \left[\varepsilon_{rr} + \upsilon(\varepsilon_{\theta\theta} + \varepsilon_{zz}) - (1 + \upsilon) \alpha \Delta T \right] \tag{44}$$

$$\sigma_{\theta\theta} = \frac{\mathrm{E}}{1 - \upsilon^2} \left[\varepsilon_{\theta\theta} + \upsilon(\varepsilon_{zz} + \varepsilon_{rr}) - (1 + \upsilon) \alpha \Delta T \right] \tag{45}$$

$$\sigma_{zz} = \frac{\mathrm{E}}{1 - \upsilon^2} \left[\varepsilon_{zz} + \upsilon(\varepsilon_{rr} + \varepsilon_{\theta\theta}) - (1 + \upsilon) \alpha \Delta T \right] \tag{46}$$

ΔT is the temperature rise at the radius r above the initial value

Strain –displacement equation

$$\varepsilon_{rr} = \frac{\partial u}{\partial r} \tag{47}$$

$$\varepsilon_{\theta\theta} = \frac{u}{r} \tag{48}$$

$$\varepsilon_{zz} = 0 \quad \text{(Plain-strain conditions)} \tag{49}$$

For the work-roll, we have

$$\sigma_{rr} = \frac{-\alpha E}{(1-\upsilon)} \frac{1}{r^2} \int_0^r \Delta T r dr + \frac{1}{r_0^2} \int_0^{r_0} \Delta T r dr \tag{50}$$

$$\sigma_{\theta\theta} = \frac{\alpha E}{(1-\upsilon)} \left(\frac{1}{r^2} \int_0^r \Delta T r dr + \frac{1}{r_0^2} \int_0^{r_0} \Delta T r dr - \Delta T \right) \tag{51}$$

$$\sigma_{zz} = \begin{cases} \dfrac{\mathrm{E}\alpha}{(1-\upsilon)} \left(\dfrac{2\upsilon}{r_0^2} \displaystyle\int_0^{r_0} \Delta T r dr - \Delta T \right), & \varepsilon = 0 \\ \dfrac{\mathrm{E}\alpha}{(1-\upsilon)} \left(\dfrac{2}{r_0^2} \displaystyle\int_0^{r_0} \Delta T r dr - \Delta T \right), & \varepsilon = \varepsilon_\theta \end{cases} \tag{52}$$

$$\sigma_{r\theta} = 0 \tag{53}$$

where

$$\Delta T = T(r, \theta, t) - T_a \tag{54}$$

2.5. Method of Solution

Since they have been applied to various linear and non-linear differential equations in literatures, numerical methods like the FDM (finite difference method), FEM (finite element method), and FVM (finite volume method) can be used to solve differential equations with single and multiple independent variables. An effective method of establishing a temperature profile for steady heat transfer systems is the numerical solution of FDM. By segmenting the complicated body into manageable domains, the FDM can be utilized to solve any complex body. Additionally, choosing finer grids that demand advanced computer power can significantly reduce approximation mistakes. Thus, FDM is used in this paper. The non-linear ordinary differential equations (equations (9) and (18)) must be solved using boundary conditions. Since the equations are nonlinear and depend on temperature, an accurate solution is not feasible for this set of equations. Han et al. (2005) previously emphasized the usefulness and accuracy of FDM when analyzing non-linear situations. Therefore, in this work, FDM is used to discretize the governing equations (9) and (18) along with the boundary conditions.

$$\frac{\partial^2 T}{\partial x^2} = \frac{T_{i+1,j}^{n+1} - 2T_{i,j}^{n+1} + T_{i-1,j}^{n+1} + T_{i+1,j}^{n} - 2T_{i,j}^{n} + T_{i-1,j}^{n}}{2(\Delta x)^2} \tag{55}$$

$$\frac{\partial^2 T}{\partial y^2} = \frac{T_{i,j+1}^{n+1} - 2T_{i,j}^{n+1} + T_{i,j-1}^{n+1} + T_{i,j+1}^{n} - 2T_{i,j}^{n} + T_{i,j-1}^{n}}{2(\Delta y)^2} \tag{56}$$

$$\frac{\partial^2 T}{\partial r^2} = \frac{T_{k+1,l}^{n+1} - 2T_{k,l}^{n+1} + T_{k-1,l}^{n+1} + T_{k+1,l}^{n} - 2T_{k,l}^{n} + T_{k-1,l}^{n}}{2(\Delta r)^2} \tag{57}$$

$$\frac{\partial^2 T}{\partial \theta^2} = \frac{T_{k,l+1}^{n+1} - 2T_{k,l}^{n+1} + T_{k,l-1}^{n+1} + T_{k,l+1}^{n} - 2T_{k,l}^{n} + T_{k,l-1}^{n}}{2(\Delta \theta)^2} \tag{58}$$

$$\frac{\partial T}{\partial x} = \frac{T_{i+1,j}^{n+1} - T_{i-1,j}^{n+1} + T_{i+1,j}^{n} - T_{i-1,j}^{n}}{4(\Delta x)} \tag{59}$$

$$\frac{\partial T}{\partial y}=\frac{T_{i,j+1}^{n+1}-T_{i,j-1}^{n+1}+T_{i,j+1}^{n}-T_{i,j-1}^{n}}{4(\Delta y)} \tag{60}$$

$$\frac{\partial^2 T}{\partial r^2}=\frac{T_{m+1,l}^{n+1}-2T_{m,l}^{n+1}+T_{m-1,l}^{n+1}+T_{m+1,l}^{n}-2T_{m,l}^{n}+T_{m-1,l}^{n}}{2(\Delta r)^2} \tag{61}$$

$$\frac{\partial^2 T}{\partial \theta^2}=\frac{T_{m,l+1}^{n+1}-2T_{m,l}^{n+1}+T_{m,l-1}^{n+1}+T_{m,l+1}^{n}-2T_{m,l}^{n}+T_{m,l-1}^{n}}{2(\Delta \theta)^2} \tag{62}$$

$$\frac{\partial T}{\partial r}=\frac{T_{m+1,l}^{n+1}-T_{m-1,l}^{n+1}+T_{m+1,l}^{n}-T_{m-1,l}^{n}}{4(\Delta r)} \tag{63}$$

$$\frac{\partial T}{\partial \theta}=\frac{T_{m,l+1}^{n+1}-T_{m,l-1}^{n+1}+T_{m,l+1}^{n}-T_{m,l-1}^{n}}{4(\Delta \theta)} \tag{64}$$

$$\frac{\partial T}{\partial t}=\frac{T_{i,j}^{n+1}-T_{i,j}^{n}}{(\Delta t)}=\frac{T_{m,l}^{n+1}-T_{m,l}^{n}}{(\Delta t)} \tag{65}$$

When the aforementioned finite difference schemes are substituted into equations (9) and (18), the equivalent finite difference schemes are obtained as

$$\begin{aligned}&\frac{\partial\left(\rho c_p(T)T\right)}{\partial t}+\left(\frac{u_m h_m}{h}\right)\frac{\partial\left(\rho c_p(T)T\right)}{\partial x}-\frac{yu_0}{h}\frac{d}{dx}\left(\frac{h_0}{h}\right)\frac{\partial\left(\rho c_p(T)T\right)}{\partial y}=\frac{\partial}{\partial x}\left(k(T)\frac{\partial T}{\partial x}\right)+\frac{\partial}{\partial y}\left(k(T)\frac{\partial T}{\partial y}\right)\\&+\eta\left(\sigma_0+B\left(\int_0^L\left(\frac{h(x)\dot{\bar{\varepsilon}}}{u_m h_m}\right)dx\right)^p\right)\dot{\bar{\varepsilon}}+m|u_r|Ak_s\sqrt{\frac{h_f}{R}}\frac{ln\left(\frac{h_o}{h_f}\right)+\frac{1}{4}\sqrt{\frac{h_f}{R}}\sqrt{\left(\frac{h_o}{h_f}\right)-1}\left[\frac{-2}{\pi}arctan\left(\frac{|u_r|}{a}\right)\right]}{arctan\left(\sqrt{\left(\frac{h_o}{h_f}\right)-1}\right)}\end{aligned} \tag{66}$$

Then, the thermal model for the rolled material is given as

$$\begin{aligned}&\rho\left[\left(T\cdot\frac{\partial c_p}{\partial T}\cdot\frac{\partial T}{\partial t}\right)+c_p\frac{\partial T}{\partial t}\right]+\rho\left(\frac{u_m h_m}{h}\right)\left[\left(T\cdot\frac{\partial c_p}{\partial T}\cdot\frac{\partial T}{\partial x}\right)+c_p\frac{\partial T}{\partial x}\right]+\rho\frac{yu_0h_0}{h^3}\frac{dh}{dx}\left[\left(T\cdot\frac{\partial c_p}{\partial T}\cdot\frac{\partial T}{\partial y}\right)+c_p\frac{\partial T}{\partial y}\right]\\&=k\left(\frac{\partial^2 T}{\partial x^2}\right)+\left(\frac{\partial k}{\partial x}\cdot\frac{\partial T}{\partial x}\right)+k\left(\frac{\partial^2 T}{\partial y^2}\right)+\left(\frac{\partial k}{\partial y}\cdot\frac{\partial T}{\partial y}\right)+\eta\left(\sigma_0+B\left(\frac{\dot{\bar{\varepsilon}}}{u_m h_m}\right)^p\left(\int_0^L h(x)dx\right)^p\right)\dot{\bar{\varepsilon}}\\&+m|u_r|Ak_s\sqrt{\frac{h_f}{R}}\frac{ln\left(\frac{h_o}{h_f}\right)+\frac{1}{4}\sqrt{\frac{h_f}{R}}\sqrt{\left(\frac{h_o}{h_f}\right)-1}\left[\frac{-2}{\pi}arctan\left(\frac{|u_r|}{a}\right)\right]}{arctan\left(\sqrt{\left(\frac{h_o}{h_f}\right)-1}\right)}\end{aligned} \tag{67}$$

Which can be written as

$$\begin{aligned}&\rho\left(T\cdot\frac{\partial c_p}{\partial T}+c_p\right)\frac{\partial T}{\partial t}+\rho\left(\frac{u_m h_m}{h}\right)\left[\left(T\cdot\frac{\partial c_p}{\partial T}\right)+c_p\right]\frac{\partial T}{\partial x}+\rho\frac{yu_0h_0}{h^3}\frac{dh}{dx}\left[\left(T\cdot\frac{\partial c_p}{\partial T}\right)+c_p\right]\frac{\partial T}{\partial y}\\&=k\left(\frac{\partial^2 T}{\partial x^2}\right)+\left(\frac{\partial k}{\partial T}\cdot\frac{\partial T}{\partial x}\right)\frac{\partial T}{\partial x}+k\left(\frac{\partial^2 T}{\partial y^2}\right)+\left(\frac{\partial k}{\partial T}\cdot\frac{\partial T}{\partial y}\right)\frac{\partial T}{\partial y}+\eta\left(\sigma_0+B\left(\frac{\dot{\bar{\varepsilon}}}{u_m h_m}\right)^p\left(\int_0^L h(x)dx\right)^p\right)\dot{\bar{\varepsilon}}\\&+m|u_r|Ak_s\sqrt{\frac{h_f}{R}}\frac{ln\left(\frac{h_o}{h_f}\right)+\frac{1}{4}\sqrt{\frac{h_f}{R}}\sqrt{\left(\frac{h_o}{h_f}\right)-1}\left[\frac{-2}{\pi}arctan\left(\frac{|u_r|}{a}\right)\right]}{arctan\left(\sqrt{\left(\frac{h_o}{h_f}\right)-1}\right)}\end{aligned} \tag{68}$$

The thermal model for the rolled material's finite difference scheme is stated as

$$\rho\left(T_{i,j}^{n}\cdot\left(\frac{\partial c_p}{\partial T}\right)_{i,j}^{n}+\left(c_p\right)_{i,j}^{n}\right)\left(\frac{T_{i,j}^{n+1}-T_{i,j}^{n}}{(\Delta t)}\right)+\rho\left(\frac{u_m h_m}{h}\right)\left(T_{i,j}^{n}\cdot\left(\frac{\partial c_p}{\partial T}\right)_{i,j}^{n}+\left(c_p\right)_{i,j}^{n}\right)\left(\frac{T_{i+1,j}^{n+1}-T_{i-1,j}^{n+1}+T_{i+1,j}^{n}-T_{i-1,j}^{n}}{4(\Delta x)}\right)$$
$$+\rho\frac{yu_0h_0}{h^3}\left(\frac{h_{i+1,j}-h_{i-1,j}}{2(\Delta x)}\right)\left(T_{i,j}^{n}\cdot\left(\frac{\partial c_p}{\partial T}\right)_{i,j}^{n}+\left(c_p\right)_{i,j}^{n}\right)\left(\frac{T_{i,j+1}^{n+1}-T_{i,j-1}^{n+1}+T_{i,j+1}^{n}-T_{i,j-1}^{n}}{4(\Delta y)}\right)$$
$$=\left(k\right)_{i,j}^{n}\left(\frac{T_{i+1,j}^{n+1}-2T_{i,j}^{n+1}+T_{i-1,j}^{n+1}+T_{i+1,j}^{n}-2T_{i,j}^{n}+T_{i-1,j}^{n}}{2(\Delta x)^2}\right)+\left(\left(\frac{\partial k}{\partial T}\right)_{i,j}\cdot\left(\frac{T_{i+1,j}^{n+1}-T_{i-1,j}^{n+1}+T_{i+1,j}^{n}-T_{i-1,j}^{n}}{4(\Delta x)}\right)\right)\left(\frac{T_{i+1,j}^{n+1}-T_{i-1,j}^{n+1}+T_{i+1,j}^{n}-T_{i-1,j}^{n}}{4(\Delta x)}\right)$$
$$+\left(k\right)_{i,j}^{n}\left(\frac{T_{i,j+1}^{n+1}-2T_{i,j}^{n+1}+T_{i,j-1}^{n+1}+T_{i,j+1}^{n}-2T_{i,j}^{n}+T_{i,j-1}^{n}}{2(\Delta y)^2}\right)+\left(\left(\frac{\partial k}{\partial T}\right)_{i,j}\cdot\left(\frac{T_{i,j+1}^{n+1}-T_{i,j-1}^{n+1}+T_{i,j+1}^{n}-T_{i,j-1}^{n}}{4(\Delta y)}\right)\right)\left(\frac{T_{i,j+1}^{n+1}-T_{i,j-1}^{n+1}+T_{i,j+1}^{n}-T_{i,j-1}^{n}}{4(\Delta y)}\right) \quad (69)$$
$$+\eta\left(\sigma_0+B\left(\frac{\dot{\bar{\varepsilon}}}{u_n h_n}\right)^{n}\left(\sum_{0}^{L}h(x)\right)^{n}\right)\dot{\bar{\varepsilon}}$$
$$+m\left|u_r\right|Ak_s\sqrt{\frac{h_f}{R}}\frac{ln\left(\frac{h_o}{h_f}\right)+\frac{1}{4}\sqrt{\frac{h_f}{R}}\sqrt{\left(\frac{h_o}{h_f}\right)-1}\left[\frac{-2}{\pi}arctan\left(\frac{\left|u_r\right|}{a}\right)\right]}{arctan\left(\sqrt{\left(\frac{h_o}{h_f}\right)-1}\right)}$$

The initial condition is

$$n=0,\ T_{i,j}^{0}=T_o\ \ at\ \ i=1,2,3,.....M,\ \ j=1,2,3,.....N \quad (70)$$

The horizontal symmetry plane's thermal boundary condition is

$$n>0,\ T_{i,1}^{n}=T_{i,0}^{n}\ \ at,\ \ i=1,2,3,...,M \quad (71)$$

On the upper surface of the roll, where the material comes into contact with the deformation zone

$$n>0,,\ T_{i,N}^{n}=T_{i,N-1}^{n}-\frac{\Delta y}{k_{i,j}^{n}}h_c\left(T_{i,N}^{n}-T_{k,l}^{n}\right)-\eta\dot{q}_{fric.}\ \ at\ \ y=y_R,\ \ at,\ \ i=1,2,3,...,M \quad (72)$$

Where

$$\dot{q}_{fric}=m\left|u_r\right|Ak_s\sqrt{\frac{h_f}{R}}\frac{ln\left(\frac{h_o}{h_f}\right)+\frac{1}{4}\sqrt{\frac{h_f}{R}}\sqrt{\left(\frac{h_o}{h_f}\right)-1}\left[\frac{-2}{\pi}arctan\left(\frac{\left|u_r\right|}{a}\right)\right]}{arctan\left(\sqrt{\left(\frac{h_o}{h_f}\right)-1}\right)}$$

Where the material comes into touch with the air at the upper surface of the rolled material

$$n>0,\ T_{i,N_{surface}}^{n}=T_{i,(N-1)_{surface}}^{n}-\frac{\Delta y}{k_{i,j}^{n}}h_c\left(T_{i,N_{surface}}^{n}-T_a\right)\ \ at\ \ y=y_{surface},\ \ at,\ \ i=1,2,3,...,M \quad (73)$$

Boundary conditions at the entrance into the roll

$$n>0,\ T_{0,j}^{n}=T_0\ \ at\ \ j=1,2,3,.....N \quad (74)$$

Boundary conditions at the exit from the roll

$$n>0,\ T_{M,j}^{n}=T_{M-1,j}^{n}\ \ at\ \ j=1,2,3,.....N \quad (75)$$

By expanding the work-roll thermal model

$$\rho_r\left[\left(T\cdot\frac{\partial c_{p,r}}{\partial T}\cdot\frac{\partial T}{\partial t}\right)+c_{p,r}\frac{\partial T}{\partial t}\right]+\omega\rho_r\left[\left(T\cdot\frac{\partial c_{p,r}}{\partial T}\cdot\frac{\partial T}{\partial\theta}\right)+c_{p.r}\frac{\partial T}{\partial\theta}\right]$$
$$=k_r\frac{\partial^2T}{\partial r^2}+\frac{k_r}{r}\frac{\partial T}{\partial r}+\frac{1}{r}\frac{\partial k}{\partial r}\frac{\partial T}{\partial r}+\frac{k_r}{r^2}\frac{\partial^2T}{\partial\theta^2}+\frac{1}{r^2}\frac{\partial k}{\partial\theta}\frac{\partial T}{\partial\theta} \quad (76)$$

Which can also be written as

$$\rho_r\left(T_{m,l}^n\cdot\left(\frac{\partial c_{p,r}}{\partial T}\right)_{m.l}^n+\left(c_{p,r}\right)_{m,l}^n\right)\left(\frac{T_{m,l}^{n+1}-T_{m,l}^n}{(\Delta t)}\right)+\omega\rho_r\left(T_{m,l}^n\cdot\left(\frac{\partial c_p}{\partial T}\right)_{m,l}^n+\left(c_{p,r}\right)_{m,l}^n\right)\left(\frac{T_{m+1,l}^{n+1}-T_{m-1,l}^{n+1}+T_{m+1,l}^n-T_{m-1,l}^n}{4(\Delta\theta)}\right)$$
$$=\left(k_r\right)_{m,l}^n\left(\frac{T_{m+1,l}^{n+1}-2T_{m,l}^{n+1}+T_{m-1,l}^{n+1}+T_{m+1,l}^n-2T_{m,l}^n+T_{m-1,l}^n}{2(\Delta r)^2}\right)+\frac{\left(k_r\right)_{m,l}^n}{m\Delta r}\left(\frac{T_{m+1,l}^{n+1}-T_{m-1,l}^{n+1}+T_{m+1,l}^n-T_{m-1,l}^n}{4(\Delta r)}\right)$$
$$+\frac{1}{r}\left(\left(\frac{\partial k}{\partial T}\right)_{m,j}^n\cdot\left(\frac{T_{m+1,l}^{n+1}-T_{m-1,l}^{n+1}+T_{m+1,l}^n-T_{m-1,l}^n}{4(\Delta r)}\right)\right)\left(\frac{T_{m+1,l}^{n+1}-T_{m-1,l}^{n+1}+T_{m+1,l}^n-T_{m-1,l}^n}{4(\Delta r)}\right)$$
$$+\frac{\left(k_r\right)_{m,l}^n}{(m\Delta r)^2}\left(\frac{T_{m,l+1}^{n+1}-2T_{m,l}^{n+1}+T_{m,l-1}^{n+1}+T_{m,l+1}^n-2T_{m,l}^n+T_{m,l-1}^n}{2(\Delta\theta)^2}\right)$$
$$+\frac{1}{(m\Delta r)^2}\left(\left(\frac{\partial k}{\partial T}\right)_{m,j}^n\cdot\left(\frac{T_{m,l+1}^{n+1}-T_{m,l-1}^{n+1}+T_{m,l+1}^n-T_{m,l-1}^n}{4(\Delta\theta)}\right)\right)\left(\frac{T_{m,l+1}^{n+1}-T_{m,l-1}^{n+1}+T_{m,l+1}^n-T_{m,l-1}^n}{4(\Delta\theta)}\right)$$

The initial boundary condition is

$$t=0,\ T=T_o\ \ at\ \ 0\le r\le r_o,\ 0\le\theta\le 2\pi\ \ (77)$$

The horizontal symmetry plane's thermal boundary condition is

$$t>0,\ \frac{\partial T}{\partial y}=0\ \ at\ \ y=0,\ 0\le x\le L \tag{78}$$

The input heat flux that travels from the strip contact area to the work-roll is given as

$$t>0,\ -k(T)\frac{\partial T}{\partial r}=h_c\left(T-T_s\right)-\eta\dot{q}_{fric}\ \ at\ \ r=r_{surface},\ 0\le\theta\le 2\pi \tag{79}$$

T_s is the temperature of the strip surface, obtained by solving the thermal issue presented by the strip, while T is the surface temperature of the work-roll. The work roll cools down due to exposure to the environment, which is taken into account on the work roll's free surface. Due to the roll and air making contact, the input heat flux that is transported from the roll to the air is

$$t>0,\ -k(T)\frac{\partial T}{\partial r}=h\left(T-T_a\right)\ \ at\ \ r=r_{surface},\ 0\le\theta\le 2\pi \tag{80}$$

At the work-roll's outside layer

$$t>0,\ T=T_o\ \ at\ \ r=r^*,\ 0\le\theta\le 2\pi \tag{81}$$

$$\sigma_x=\sigma_y=\frac{\alpha E}{1-\nu}\left[-\Delta T+\frac{1}{h_n}\int_{-h/2}^{h/2}\Delta T dz+\frac{12z}{h_n^3}\int_{-h/2}^{h/2}\Delta T z dz\right] \tag{82}$$

For the work-roll, we have

$$\sigma_{rr}=\frac{-\alpha E}{(1-\upsilon)}\frac{1}{r^2}\int_0^r\Delta T r dr+\frac{1}{r_0^2}\int_0^{r_0}\Delta T r dr \tag{83}$$

$$\sigma_{\theta\theta}=\frac{\alpha E}{(1-\upsilon)}\left(\frac{1}{r^2}\int_0^r\Delta T r dr+\frac{1}{r_0^2}\int_0^{r_0}\Delta T r dr-\Delta T\right) \tag{84}$$

$$\sigma_{zz}=\begin{cases}\dfrac{\mathrm{E}\alpha}{(1-\upsilon)}\left(\dfrac{2\upsilon}{r_0^2}\displaystyle\int_0^{r_0}\Delta T r dr-\Delta T\right), & \varepsilon=0\\[2ex] \dfrac{\mathrm{E}\alpha}{(1-\upsilon)}\left(\dfrac{2}{r_0^2}\displaystyle\int_0^{r_0}\Delta T r dr-\Delta T\right), & \varepsilon=\varepsilon_\theta\end{cases} \tag{85}$$

$$\sigma_{r\theta}=0 \tag{86}$$

3. RESULTS AND DISCUSSION

3.1. Grid independence Test

To reduce computation error, the strip's sensitive zone, or deformation zone, is tested for grid independence. When the grid points reach 24000 or more, there is little difference in the results regardless of the number of grids or grid points. As a result, the grid independent solution is based on the results from 24000 grid points.

3.2. Impacts of rolling parameters on the work roll surface and strip temperature

Figure 5–10 depict the effects of parameters of rolling on the work-roll surface and temperature of strip. Figure 5 depicts the variance of work-roll surface temperature variation with the angular location during deforming and cooling. It demonstrates how the work-roll's surface temperature varies with the roll's angular position within the deformation zone. This is due to the fact that the deformation energy produced in the deformation zone grows as the angular position does. Additionally, as a result of this, the deformation zone experiences high strain rates, frictional stresses, and heat production, which raises temperature. Additionally, as depicted in the image, note that throughout the cooling process, the work-roll surface temperature decreases with angular position. As the deformed strip emerges from the deformation zone, its temperature decreases due to the presence of cooled ambient air, which has a lower temperature. The work-roll surface temperature variation over time is seen in Figure 6. The temperature history during the rolling operation follows the same trend as in the case of the angular position. As the rolling process is prolonged, the strain rate, frictional stress, and heat produced within the deformation zone increase, resulting in an increase in surface temperature of the rollers.

Figure 7 illustrates the impacts of strip velocity on strip surface temperature, whereas Figure 8 illustrates the impacts of strip thickness or strip depth on strip temperature. Graphs demonstrate that while strip temperature increases with strip velocity, it decreases as strip depth increases. Figure 9 demonstrates how the work-roll surface temperature rises with work-roll angular velocity and Figure 10 demonstrates the work-roll surface temperature's parabolic behavior with barrel length, it is discovered that the strip's interior temperature rises uniformly throughout the roll at low speeds of rolling, with the greatest temperature occurring in the centerline region of the strip. This is due to the deformation energy piling up (accumulating). However, as rolling speed increases, a significant portion of energy is transported together with the material through transfer of heat by convection in the heat equation. As a result, the greatest strip temperature is moved toward the upper surface from the centerline region.

The stresses alterations at the roll surface over time are depicted in Figure 11. In less than a second, as shown in the picture, the compressive tension at the beginning of idling changes to tensile stress. The period from the start of idling to 5.0 s was enlarged as indicated in Figure 12, and the resulting circumferential stresses are shown in Figure 13 to study the change to tensile stress from compressive stress. In contrast to some other studies' findings, the figure demonstrates that because the beginning temperature of the roll in this study was fixed at 30°C, no tension due to tensile was formed in the roll when rolling. Figure 14 shows the variation in stress on the surface of the for a single rotation. On the roll surface, compressive stress predominated initially, but when the initial roll temperature rose, tensile tension began to develop.

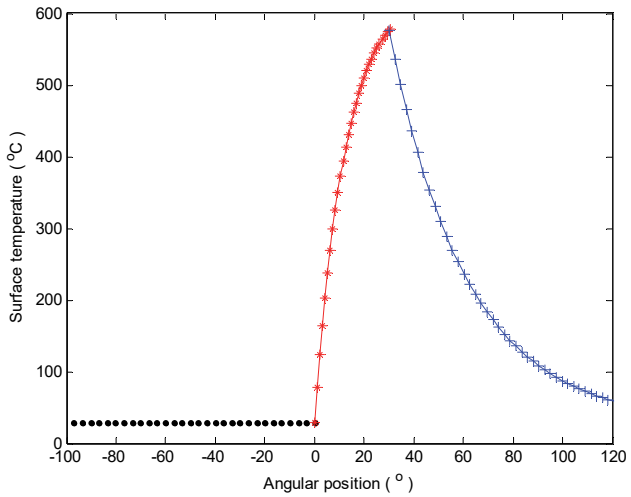

Figure 5: Variation of work-roll surface temperature variation with the angular position

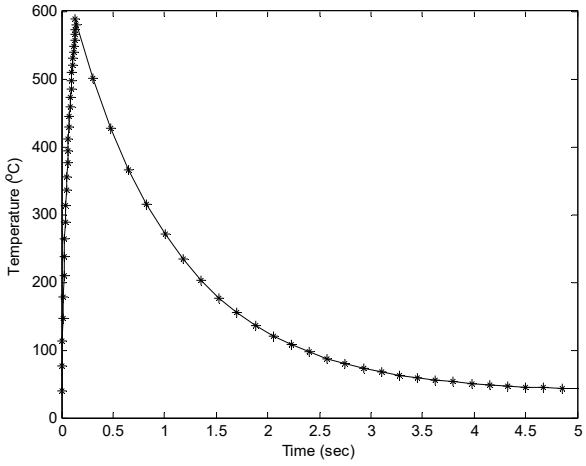

Figure 6: Variation of work-roll surface temperature variation with time

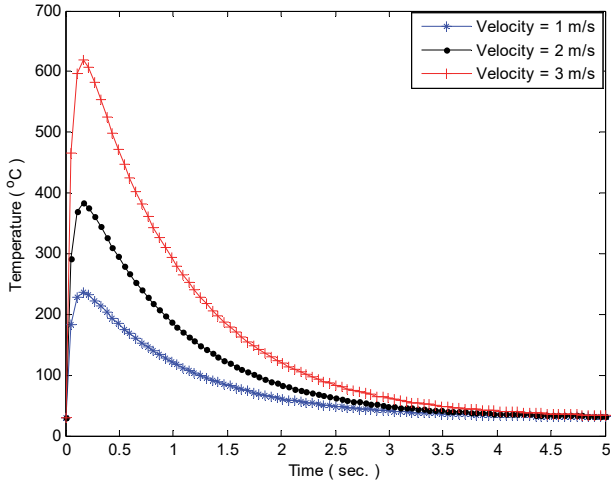

Figure 7: Effects of strip velocity on the work-roll surface temperature

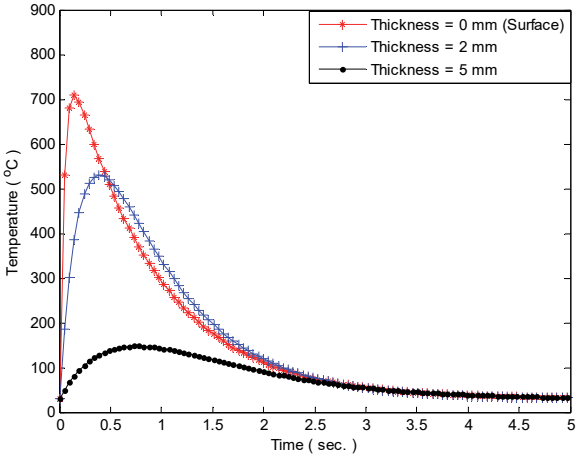

Figure 8: Strip temperature at different thickness

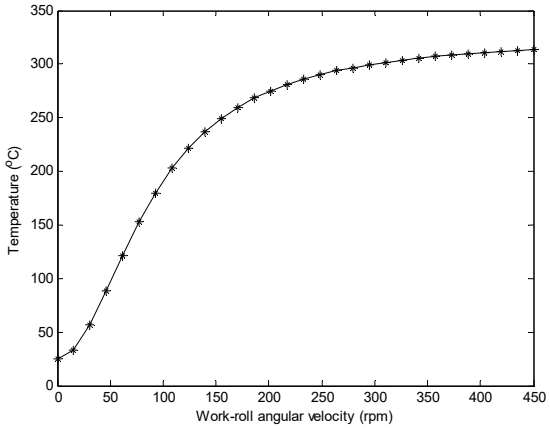

Figure 9: Work-roll surface temperature variation with work-roll angular velocity

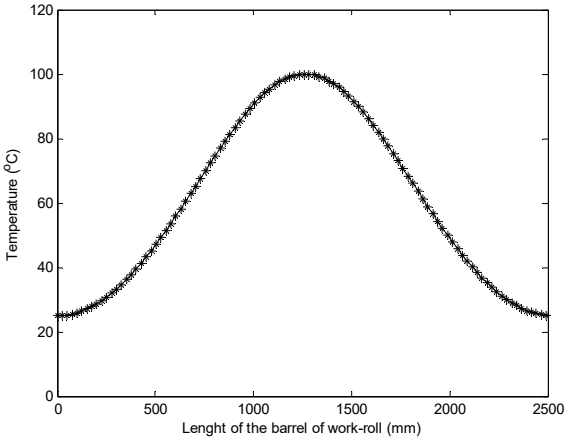

Figure 10: Work-roll surface temperature variation with the length of the barrel

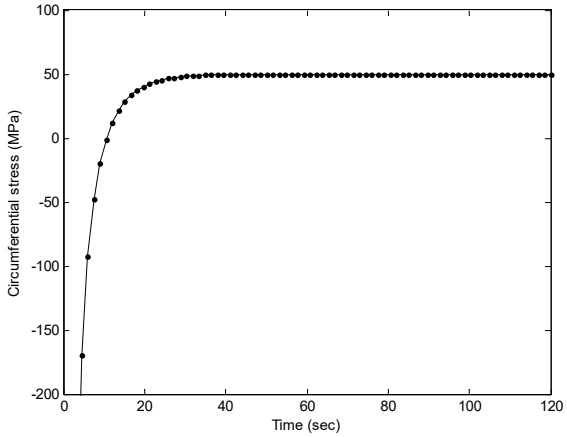

Figure 11: Circumferential stress variation with time until steady-state

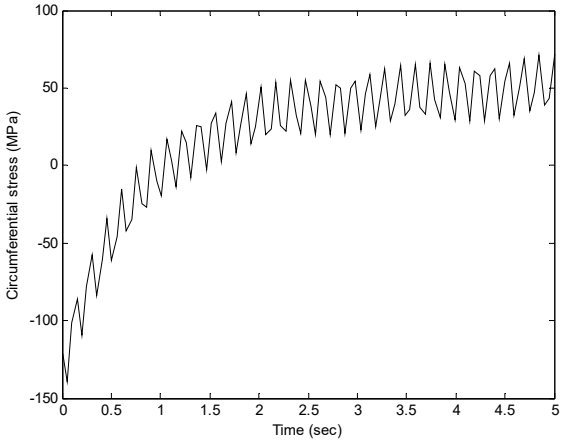

Figure 12: Circumferential stress variation with time form 0 s to 5.0 s

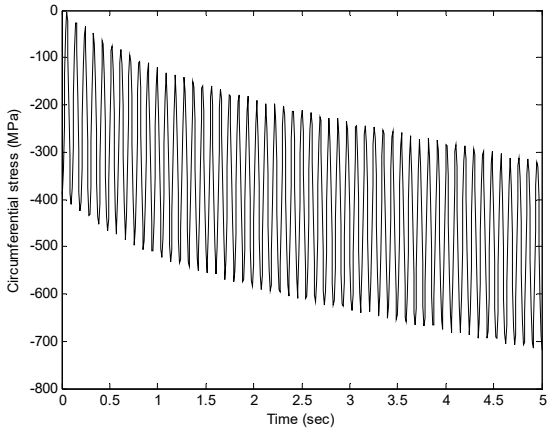

Figure 13: Circumferential stress variation with time

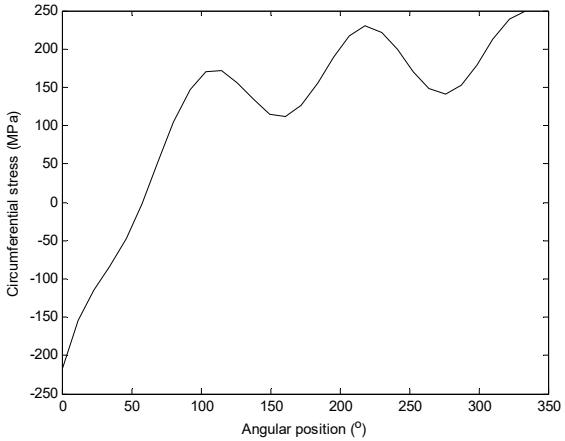

Figure 14: Circumferential stress variation with angular position

3.3. Impact of percentage drop on the strip's temperature distribution

With the help of numerical models, we can predict how rolling parameters will affect thermal strips and work-rolls' thermal performance during rolling. Temperature contour plots (Figure 15) only display one half of geometry, due to the symmetry of the rolling process. The findings demonstrate as predicted that when the strip contacts the roll, its temperature starts to rise because of the frictional heat produced as a result of contact. Furthermore, the strip begins to deform once it enters the bite region, and the heat produced by the deformation raises the surface temperature of the workpiece to a specific value as indicated in the picture. At high speed, the strip and roll touches for a comparatively less amount of time; therefore, the roll absorbs less heat, while the strip absorbs significant amount of heat energy. Some parametric experiments are conducted with the goal of examining the impact of different parameters on the transfer of heat trend throughout the rolling process. The effect of operation speed (rolling) and percentage drop in the temperature distribution in the strip's deformation region, as depicted in Figure 15. Graphs demonstrate the distributions of temperature in the deformation area for reductions of 10%, 20%, and 40% for rolling speeds of 40, 50, and 60 rpm, respectively. The findings indicate that as strip thickness is reduced and rolling speed rises, the temperature in the deformation zone rises. This is because the time of contact with the work-rolls lowers and generated deformation energy in the deformation zone increases as the percentage attrition in strip thickness and the rolling speed rise. Due to this, the deformation zone produces high levels of strain rate, frictional stress, and heat, which raises the temperature. By increasing the percentage reduction in the rolling process from 20% to 40%, the distribution of temperature in the work-roll is greatly affected. The temperature in the bite region rises substantially to a value compared to the non-bite region. With increasing rotational speeds of the work-roll, the strips' isotherms also move toward the outlet of the biting region. This demonstrates how the hot zone grows in the direction of the material flow. As a result, as seen in Figure 15, the high-temperature zone moves from the strip's center to its top section. With fast rotation speeds, the roll has less time to come in contact with the deforming workpiece (a strip), which reduces thermal penetration in the roll. As observed in the figure, the deformation zone's hottest area occurs close to the exit zone and the strip mall during the hot rolling operation. This is so because it is here where tension and stress are at their maximum levels. As strip thickness decreases, the surface of the deforming material and the region of the highest temperature shifts closer to the. It should be noted that when the percentage of the strip's decrease surpasses a particular threshold, a greater amount of heat is generated at the strip-roll interface.

a) rolling speed of 60rpm and 10% reduction

b) rolling 60rpm and 20% reduction

Figure 15: Distributions of temperature in the deformation at a rolling speed of 60rpm, 50 rpm, 40rpm and 10%, 20% , 40% reduction

c) rolling speed of 60rpm and 40% reduction

d) rolling speed of 50rpm and 10% reduction

e) rolling speed of 50rpm and 20% reduction

f) rolling speed of 50rpm and 40% reduction

g) a rolling speed of 40rpm and 10% reduction

h) rolling speed of 40rpm and 20% reduction

i) Rolling speed of 40rpm and 40% reduction

Figure 15: Distributions of temperature in the deformation
at a rolling speed of 60rpm, 50 rpm, 40rpm and 10%, 20% , 40% reduction

4. CONCLUSION

This project uses the finite difference approach to analyze the thermal stress and how temperature is distributed in the roll and strip when carrying out the hot rolling. The metal process is subjected to parametric analysis, with the following findings:

1) As the proportion of how thick the strip is reducing, and the rolling speed rises, the temperature in the deformation zone rises.
2) Increment in percentage reduction from 20% to 40%, significantly affects how temperature is distributed in the work roll.
3) When the rotational speeds of the work-roll increases, the strips' isotherms move toward the outlet of the biting region.
4) The greatest temperature region shifts to areas closer to the deforming material's surface as the percentage reduction in strip thickness rises.

5) When the percentage of the strip's reduction surpasses a particular threshold, the heat generation on strip-roll contact significantly increases.
6) The temperature of the strip rises with velocity but falls as the strip's depth increases.
7) The temperature of the surface increases with increase in the work-roll angular velocity.
8) The temperature of the strip at its maximum occurs in the strip centerline region at moderate rolling speeds, and the temperature increase within the strip is uniform.

ACKNOWLEDGEMENTS

The authors acknowledged the support of University of Lagos.

REFERENCES

[1] F. J. Humphreys and M. Hatherly, “Recrystallization and Related Annealing Phenomena”, Elsevier Science, Oxford (UK), (1996)

[2] G. E. Dieter, “Mechanical Metallurgy”, McGraw-Hill, New York (USA), (1987)

[3] M. Pietrzyk and J. G. Lenard, “A study of heat transfer during flat rolling”, Int J. Numer. Methods Eng, Vol. 30(8), pp. 1459-1469, https://doi.org/10.1002/nme.1620300809, (1990)

[4] C. Bertrand-Corsini, C. David, A. Bern, P. Montmitonnet, J. L. Chenot, P. Buessler and F. Fau, "A three dimensional thermomechanical analysis of steady flows in hot forming processes: applications to hot flat rolling and hot shape rolling", In: Modelling of Metal Forming Processes, J. L. Chenot and E. Oñate, Eds. Springer, Dodrecht (Netherlands), pp. 271-279, (1988)

[5] G. F. Bryant and M. O. Heselton, "Roll gap temperature models for hot mills", Metals Technology, Vol. 9(1), pp. 469-477, https://doi.org/10.1179/030716982803285792, (1982)

[6] G. F. Bryant and T. S. L. Chiu, "Simplified roll-temperature model: spray-cooling and stress effects", Metals Technology, Vol. 9(1), 485-492, https://doi.org/10.1179/030716982803285729, (1982)

[7] J. C. Heinrich and O. C. Zienkiewicz, "Quadratic finite element schemes for two-dimensional convective transport problems", International Journal for Numerical Methods in Engineering, Vol. 11(12), pp. 1831-1844, https://doi.org/10.1002/nme.1620111207, (1977)

[8] S. Serajzedah, A. K. Taheri, M. Nejati, J. Izadi and M. Fattahi, "An investigation on strain inhomogeneity in hot strip rolling process", Journal of Materials Processing Technology, Vol. 128(1-3), pp. 88-99, https://doi.org/10.1016/S0924-0136(02)00276-5, (2002)

[9] S. Serajzadeh, "Prediction of temperature distribution and phase transformation on the run-out table in the process of hot strip rolling", Applied Mathematical Modelling, Vol. 27(11), pp. 861-875, https://doi.org/10.1016/S0307-904X(03)00085-4, (2003)

[10] V. Nagpal, G. D. Lahoti and T. Altan, "A numerical method for simulataneous prediction of metal flow and temperature in upset forging of rings", Journal of Engineering for Industry, Vol. 100(4), pp. 413-420, https://doi.org/10.1115/1.3439455, (1978)

[11] M. J. M. Barata Marques and P. A. F. Martins, "The use of dual-stream functions in the analysis of three dimensional metal forming processes", International Journal of Mechanical Sciences, Vol. 33(4), pp. 313-323, https://doi.org/10.1016/0020-7403(91)90043-3, (1991)

[12] S. G. Chung, K. Kuwahara and O. Richmond, "Streamline-coordinate finite-difference merthod for hot metal deformations", Journal of Computational Physics, Vol. 108(1), pp. 1-7, https://doi.org/10.1006/jcph.1993.1157, (1993)

[13] F. Hollander, "A model to calculate the complete temperature distribution in steel during hot rolling", Journal of the Iron and Steel Institute, Vol. 208, pp. 46-74, (1970)

[14] K. Mori, K. Osakada and T. Oda, "Simulation of plane-strain rolling by the rigid-plastic finite element method", International Journal of Mechanical Sciences, Vol. 24(9), pp. 519-527, https://doi.org/10.1016/0020-7403(82)90044-3, (1982)

[15] Y. Hwu, and J.G. Lenard, "A finite element study of flat rolling", Journal of Engineering Materials and Technology, Vol. 110(1), pp. 22-27, https://doi.org/10.1115/1.3226004, (1988)

[16] I. Yarita, R. L. Mallett and E. H Lee, "Stress and deformation analysis of plane strain rolling process", Steel Research, Vol. 56(5), pp. 255-259, https://doi.org/10.1002/srin.198500631, (1985)

[17] S. M. Hwang and M. S. Joun, "Analysis of hot-strip rolling by a penalty rigid-viscoplastic finite element method", International Journal of Mechanical Sciences, Vol. 34(12), pp. 971-984, https://doi.org/10.1016/0020-7403(92)90066-P, (1992)

[18] S. M. Hwang, M. S. Joun and Y. H. Kang, "Finite element analysis of temperatures, metal flow, and roll pressure in hot strip rolling", Journal of Engineering for Industry, Vol. 115(3), pp. 290-298, https://doi.org/10.1115/1.2901663, (1993)

[19] C. Devadas and I. V. Samarasekara, "Heat transfer during hot rolling of steel strip", Ironmaking & steelmaking, Vol. 13, pp. 311-321, (1986)

[20] W. C. Chen, I. V. Samarasekara, A. Kumar and E. B. Hawbolt, "Mathematical modelling of heat flow and deformation during rough rolling", Ironmaking & steelmaking, Vol. 20(2), pp. 113-125, (1993)

[21] C. Devadas, D. Baragar, G. Ruddle and I. V. Samarasekara, "The thermal and metallurgical state of steel strip during hot rolling" Metall. Trans, Vol. 22, pp. 307-316, (1991)

[22] Z. C. Lin and Y. C. Cheng, "An investigation of the effect of speeds of work rolls on rolling strip", Journal of Engineering Materials and Technology, Vol. 117(3), pp. 341-346, https://doi.org/10.1115/1.2804549, (1995)

[23] J. D. Fletcher and J.H. Beynon, "Heat transfer in roll gap in hot strip rolling", Ironmaking & Steelmaking, Vol. 23(1), pp. 52-57, (1996)

[24] A. Sluzalec Jr, "A preliminary analysis of temperature within roll forging dies, using a finite element method", International Journal of Machine Tool Design and Research, Vol. 24(3), pp. 171-179, https://doi.org/10.1016/0020-7357(84)90002-7, (1984)

[25] A.A. Tseng, F.H. Lin, A. S. Gunderia and D.S. Ni, "Roll cooling and its relationship to roll life", Metallurgical Transactions A, Vol. 20, pp. 2305-2320, https://doi.org/10.1007/BF02666666, (1989)

[26] B. Gierulski and M. Ciernak, "Temperature field on strip cross-section during hot rolling". Steel Research International, Vol. 60(5), pp. 208-214, https://doi.org/10.1002/srin.198900276, (1989)

[27] A.N. Karagiozis and J.G. Lenard, "Temperature distribution in a slab during hot rolling", Journal of Engineering Materials and Technology, Vol. 110(1), pp. 17-21, https://doi.org/10.1115/1.3226002, (1988)

[28] F. Sassani and M. Xiao, "Modelling hot flat-rolling of components having curved profiles-part II. Characterization of heat transfer and flow stress", International Journal of Mechanical Sciences, Vol. 37(12), pp.1283-1293, https://doi.org/10.1016/0020-7403(95)00031-R, (1995)

[29] W.C. Chen, I.V. Samarasekera, A. Kumar and E.B. Hawbolt, "Mathematical modelling of heat flow and deformation during rough rolling", Ironmaking & steelmaking, Vol. 20(2), pp.113-125, (1993).

[30] S. Serajzedeh, "Effects of rolling parameters on work-roll temperature distribution in the hot rolling of steels", The International Journal of Advanced Manufacturing Technology, Vol. 35, pp. 859-866, https://doi.org/10.1007/s00170-006-0764-3, (2008).

[31] S. Serajzedeh, A. K. Taheri, M. Nejati, J. Izadi and M. Fattahi, "An investigation on strain inhomogeneity in hot strip rolling process", Journal of Materials Processing Technology, Vol. 128(1-3), pp. 88-99, https://doi.org/10.1016/S0924-0136(02)00276-5, (2002)

[32] S. Serajzadeh, "Prediction of temperature distribution and phase transformation on the run-out table in the process of hot strip rolling", Applied Mathematical Modelling, Vol. 27(11), pp. 861-875, https://doi.org/10.1016/S0307-904X(03)00085-4, (2003)

[33] O. Pawelski, "Calculation of the heat transfer number for hot rolling and forging", Archive for the ironworks, Wiley Online Library, Vol. 40(10), pp. 821-827, (1969)

[34] A. A. Tseng, S. X. Tong and T. C. Chen, "Thermal expansion and crown evaluations in rolling processes", Materials & Design, Vol. 17(4), pp. 193-204, https://doi.org/10.1016/S0261-3069(96)00061-1, (1996)

[35] V. B. Ginzburg, "Basic principles of customized computer models for cold and hot strip mills", Iron and Steel Engineer, Vol. 62(9), pp. 21-35, (1985)

[36] R. B. Mei, C. S. Li, X. H. Liu and B. Han, "Analysis of strip temperature in hot rolling process by finite element method", Journal of Iron and Steel Research International, Vol. 17(2), pp. 17-21, https://doi.org/10.1016/S1006-706X(10)60052-0, (2010)

[37] Z. Hadala and Z. Malinowski, "Validation of the boundary conditions in on-line temperature model for plate rolling mill", Archives of Metallurgy and Materilas, Vol. 55(2), pp. 455-461, (2010)

[38] H. B. Khadem, "Prediction of heat transfer in steel slab in rolling stand", MSc Dissertation, Department of Mechanical Engineering, Isfahan University of Technology (Iran), (1998)